AFOSR - TR - 75 - 1382

ADA015873

SYNTHESIS OF NEW SUPERHARD MATERIALS AND THEIR APPLICATION TO CUTTING TOOLS

R.F. BUNSHAH
A.H. SHABAIK

UCLA • SCHOOL OF ENGINEERING AND APPLIED SCIENCE

University of California

Los Angeles, California   90024

Semi-Annual Technical Report No. 2

SYNTHESIS OF NEW SUPERHARD MATERIALS AND THEIR APPLICATION TO CUTTING TOOLS

ARPA Order No.:	2574
Program Code:	4D10
Effective Date of Contract:	1 March 1974
Contract Expiration Date:	31 December 1975
Amount:	$160,000
Contract No.:	F44620-74-C-0044
Principal Investigator:	Professor R. F. Bunshah (213) 825-2210
Co-Princiapl Investigator:	Professor A. H. Shabaik (213) 825-5143
Program Manager:	None
Date of Report:	30 April 1975
Period of Performance:	1 September 1974 to 31 March 1975
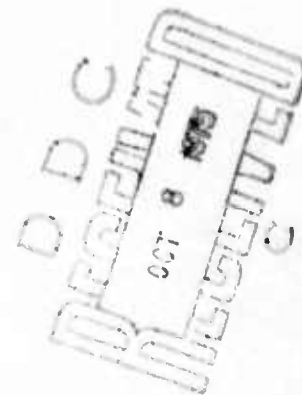
REPORT DOCUMENTATION PAGE		READ INSTRUCTIONS BEFORE COMPLETING FORM
1. REPORT NUMBER AFOSR TR - 75 - 1382	2. GOVT ACCESSION NO.	3. RECIPIENT'S CATALOG NUMBER
4. TITLE (and Subtitle) SYNTHESIS OF NEW SUPERHARD MATERIALS AND THEIR APPLICATION TO CUTTING TOOLS.		5. TYPE OF REPORT & PERIOD COVERED INTERIM Technical Rept. 1 Sept 74 — 31 Mar 75
		6. PERFORMING ORG. REPORT NUMBER UCLA-ENG-7559 Report No. 2
7. AUTHOR(s) R. F. BUNSHAH A. H. SHABAIK		8. CONTRACT OR GRANT NUMBER(s) F44620-74-C-0044 ARPA Order 2574
9. PERFORMING ORGANIZATION NAME AND ADDRESS UNIVERSITY OF CALIFORNIA, LOS ANGELES MATERIALS DEPARTMENT LOS ANGELES, CALIFORNIA 90024		10. PROGRAM ELEMENT, PROJECT, TASK AREA & WORK UNIT NUMBERS ARPAOONA AO-2574 61101E 9D10
11. CONTROLLING OFFICE NAME AND ADDRESS AIR FORCE OFFICE OF SCIENTIFIC RESEARCH/NA 1400 WILSON BOULEVARD ARLINGTON, VIRGINIA 22209		12. REPORT DATE Apr 1975
		13. NUMBER OF PAGES 51
14. MONITORING AGENCY NAME & ADDRESS(if different from Controlling Office) AFOSR TR-75-1382		15. SECURITY CLASS. (of this report) UNCLASSIFIED
		15a. DECLASSIFICATION/DOWNGRADING SCHEDULE

16. DISTRIBUTION STATEMENT (of this Report)

Approved for public release; distribution unlimited.

Semi-annual technical rept. no. 2,
1 Sep 74 - 31 Mar 75,

17. DISTRIBUTION STATEMENT (of the abstract entered in Block 20, if different from Report)

18. SUPPLEMENTARY NOTES

19. KEY WORDS (Continue on reverse side if necessary and identify by block number)

ACTIVATED REACTIVE EVAPORATION	CERMET	MACHINING
DEPOSIT	TITANIUM CARBIDE	COATINGS
CARBIDES	SYNTHESIS OF MATERIALS	COATED CUTTING TOOLS
NITRIDES	CUTTING TOOLS	TOOL LIFE
OXIDES	PERFORMANCE	

20. ABSTRACT (Continue on reverse side if necessary and identify by block number)

The process of Activated Reactive Evaporation is used to synthesize superhard materials like carbides, oxides, nitrides, ultrafine grain cermets. The deposits are characterized by hardness microstructure and lattice parameter measurements. The synthesis and characterization of various carbides in the Ta-C and W-C systems, and of TiC-Ni cermets is given.   Tools of different coating characteristics are tested for machining performance at different speeds and feeds. The machining evaluation and the selection of coatings is based on the rate of deterioration of the coating, tool temperature, and cutting forces. Tool life tests show coated high speed steel tools show a 300% improvement in tool life.

DD FORM 1 JAN 73 1473   EDITION OF 1 NOV 65 IS OBSOLETE

UNCLASSIFIED

SYNTHESIS OF NEW SUPERHARD MATERIALS AND THEIR APPLICATION TO CUTTING TOOLS

R. F. Bunshah and A. H. Shabaik
Materials Department
School of Engineering and Applied Science
University of California
Los Angeles

ABSTRACT

Two major areas of effort are encompassed:

I. <u>Synthesis of Superhard Materials</u>: The process of Activated Reactive Evaporation is used to synthesize superhard materials like carbides, oxides, nitrides, ultrafine grain cermets. The deposits are characterized by hardness microstructure and lattice parameter measurements. The synthesis and characterization of various carbides in the Ta-C and W-C systems, and of TiC-Ni cermets is given.

II. <u>Study and the Effect of Superhard Coatings on the Performance of High Speed Steel Tools</u>: Tools of different coating characteristics are tested for machining performance at different speeds and feeds. The machining evaluation and the selection of coatings is based on the rate of deterioration of the coating, tool temperature, and cutting forces. Tool life tests show coated high speed steel tools show a 300% improvement in tool life.

TABLE OF CONTENTS

LIST OF FIGURES

LIST OF TABLES

ix

I. OBJECTIVE

The objectives of this research are two-fold: Firstly, the synthesis of new superhard materials. Secondly, to examine the effect of superhard coatings on the performance of high speed steel cutting tools. Such applications as well as others, e.g., grinding tools, hard coatings for abrasion and wear resistance in engines, aircraft, tanks, metal forming machinery, dies, punches, etc., could be of great interest to the DOD.

There are several reasons for concentrating the application effort on cutting tools in general and high speed steel tools in particular. Firstly, very little work has been carried out in the application of hard carbide coatings to improve the life of high speed steel tools (single point tools, end mills, cutters, etc.) even though they form the largest single item in the tool production of cutting tools; the present mill shipments of high speed steel tools is estimated at $600 million. Secondly, the Activated Reactive Evaporation (ARE) process, recently developed at UCLA under ARPA sponsorship,[1] is uniquely suited for this purpose since the hard coating can be applied even at low substrate temperatures, i.e., about 500°C, which would still retain the substrate (high speed steel tools) in its hardened and tempered condition without softening. Competing processes such as chemical vapor deposition require that the substrate be at temperatures of 1000°C or higher for the deposition of hard compounds such as TiC which would, of course, ruin the strength and toughness of the high speed steel. Such CVD processes are commercially used today to coat TiC onto a WC-Co type carbide machining inserts which can withstand high deposition temperatures (1000°C). Hard coatings can also be laid down by sputtering; however, the deposition rates from sputtering are very slow.

1

In the Activated Reactive Evaporation process, Bunshah and his co-workers[2,3] have developed a new high rate physical vapor deposition process for the synthesis of oxides, nitrides and carbides. Furthermore, they found that by controlling the deposition temperature or by heat-treatment,[4] it was possible to change the microstructure and consequently increase the hardness of TiC from 3000 to 5400 kg/mm, a value second only to diamond (see Table I) and comparable to or better than the second hardest material known, borazon (cubic boron nitride). Moreover, TiC should cost 100 times less than borazon or diamond, which is a considerable economic incentive. Finally, high speed steel (a strong and tough material) coated with a superhard layer such as TiC or other materials, would be an ideal system to study for improved tool performance since the necessary requirements of hardness for cutting and toughness to absorb the impact loads are fulfilled by this composite system.

II. RESEARCH PROGRAM

The proposed research program is divided into the following two parts:

A. Synthesis of New Superhard Materials

The Activated Reactive Evaporation (ARE) process will be used to synthesize new superhard materials such as carbides, nitrides, oxides and two-phase alloys. The ARE is a versatile process that is capable of the following:

1) Synthesizing oxides, carbides, nitrides and possibly borides and silicides.

2) Synthesizing mixed carbides (i.e., carbides of more than one metal) of controlled composition, e.g., (TiZr)C.

3) Synthesizing mixed compounds (i.e., carbo-nitrides, oxy-carbides, etc.)

2

TABLE I

Hardness of Various Materials

| Material | Knoop Hardness (kg/mm^2) | | Wooddell Scale (relative) |
	Room Temperature	900°C	Room Temperature
Diamond	7000		43
Borazon (cubic/boron nitride)	4700		19
Samarium Borides (Sm B$_{\sim2}$) Sm B$_{\sim70}$)	3610		
Rare Earth Borides (REB$_{70}$)	3500-4000		
Titanium Carbide*	3000	400	
Hafnium Carbide*	2400	800	
Vanadium Carbide	2400	400	
Silicon Carbide	2480		14
Niobium Carbide	2200	500	
Aluminum Oxide	2100		9
Tungsten Carbide	1850	1200	
Tantalum Carbide	1700	400	
Chromium Carbide (Cr$_7$C$_3$)	1500	600	
Chromium Carbide (Cr$_{23}$C$_6$)	950	700	
Quartz	820		7

* The hardness of TiC produced by Activated Reactive Evaporation can be as high as 5400 kg/mm^2.

4) Changing the microstructure and mechanical properties by variation of process parameters, e.g., (deposition temperature).

5) Producing material ranging from full density coatings all the way to powder.

6) Producing very fine grain sizes.

7) Varying and controlling the stoichiometry of carbides and other compounds.

8) Laying down a deposit which is strongly adherent to the substrate due to a diffusion bond produced between the two.

9) Producing graded microstructures, e.g., from metal to carbide.

10) Obtaining high deposition rates for coatings (5 to 25 μ per minute) which make it an economical process.

This part of the research program will be concentrated on the synthesis and characterization of the following superhard materials:

1. Carbides

a) Carbides of tungsten since they have the highest hot hardness of all carbides.

b) HfC since it has the second highest hot hardness and has been reported to be a good cutting tool coating for machining titanium.

c) Boron carbide since it is a very hard material in current usage.

d) Mixed carbides in the system VC-TiC. Hollox[5] reports a maximum in hardness at VC-25 at.% TiC.

e) Mixed carbides in the system TiC-HfC. The TiC-20% HfC alloy has the highest reported melting point of all alloys.

f) Mixed carbides in the system TiC-ZrC. "Alloys" in this system are reported to be harder than TiC.[6] It is also an experimentally easy alloy to evaporate and will serve as a model system for studying mixed carbides.

4

2. Nitrides

The synthesis of cubic boron nitride will be attempted since past work has shown that is is possible to synthesize β-SiC[7] which is also cubic. Success would provide an alternate and possible cheaper method of producing a proven hard material.

3. Oxides

a) Al_2O_3 since this is a commercially used grinding material and will be used as a model system.

b) Mixed oxides in the system Al_2O_3-ZrO_2 to produce fine grained two-phase structures of different morphology[8] harder than the pure oxides.

4. Two-Phase Alloys

a) TiC + B and VC + B - a tenfold increase in strength has been reported due to precipitation hardening.

b) Ultrafine grained cermets-carbides in a matrix of metal or alloy in an effort to improve the toughness of the carbides. The present-day cermets have a lower limit c' 3 μ in carbide particle size. The toughness increases very rapidly as the size of the carbide becomes smaller. Such a very fine grained cermet coating would be expected to retain the cutting ability of the hard carbide while improving its resistance to fracture. Preliminary work at UCLA has shown the ability to synthesize TiC-Ni cermet coating using the ARE process. As a further step, resistance to degradation at high tool tip temperatures would be improved by substituting a more refractory metal for the ductile matrix in the cermet.

c) High temperature ultrafine grained cermets-carbides in a matrix of refractory metal to improve the hot hardness of the composite structure.

The important process variables that will be studied are:

1. Substrate temperature which affects grain size, density, particle size in two-phase alloys and residual stresses. The range of substrate temperatures to be explored is 500-1500°C.

2. Heat treatment - to study annealing effects in single phase material and to study precipitation effects where applicable.

Substrate materials will be a metal and/or ceramic. Deposit thickness will be about .001-.005" so as to assure bulk properties.

Characterization of the synthesized materials will be carried out by the following:

1. Microhardness at room and elevated temperature.

2. Chemical analysis using the microprobe, the non-dispersive detector and other analytical techniques as required.

3. Microstructure using optical, scanning electron and diffraction electron microscopy.

4. X-ray diffraction to measure precision lattice parameters, "particle size" and residual stresses. Computer programs have been developed at UCLA to handle the X-ray data.

5. Density

At the start of the project, a preliminary study will be run to explore the synthesis of the various materials followed by limited characterization (lattice parameter, microhardness and structure as a function of C/M ratio) to aid material selection for detailed studies.

B. Effect of Superhard Coatings on Cutting Tool Performance

During metal cutting, tool damage can be due to tool wear (flank and crater wear), and/or cracking along the tool face. The tool must

6

support the cutting forces at the high temperatures attained during cutting, and it must also endure the cyclic thermal stresses induced by the cutting, non-cutting cycle. Such conditions call for a tool material that is both hard and tough and resistant to wear.

During this phase of the research program, high speed steel tools will be coated initially with TiC and subsequently with other super-hard materials developed in the first part of this program. The coating will provide the necessary hardness and wear resistance while the core, which is the high speed steel tool in this case, will provide the toughness and the resistance to impact loading. Machining tests will be carried out on the coated tools at different conditions of cutting speeds, feed, and depth of cut. Intermittant as well as non-intermittant tests will be employed. The cutting forces will be measured in each case using a tool dynamometer. The tool work interface temperature and friction coefficient along the tool face will be determined. Tool damage and surface finish of the machined part will be examined. Tool life will be determined The wear process and mechanism of the different coatings will be investigated using tool-maker's microscope, scanning electron microscope techniques, and electron microprobe analyses. The crater and flank wear heights will be measured at different locations. The scanning electron microscope brings out topographical details of tool wear, cracks, and failure with more clarity and detail than one can observe with an optical microscope. While a SEM photograph provides fine details of tool surfaces, it is still necessary to have the electron microprobe analysis for identification of specific elements in the worn tool surfaces which then helps to understand

the contact interactions between workpiece and tool. Correlation between microstructure and mechanical properties of the coating and the core material to their cutting performance will also be examined. Comparison of the cutting forces, temperature, friction coefficient, surface finish of the machined part, and tool wear will be examined and correlation to the physical and mechanical properties of the different coating will be carried out.

Tool damage vs. cutting speed for a given feed and depth of cut will be compared for different tool coatings. Wear measurements will be obtained from direct comparison of the tool contours before and after test. Correlation of tool wear results to parameters characterizing the coating (coating composition, grain size, density, lattice parameter, coating thickness, microhardness and C/M ratio) will be investigated. Such correlation will constitute the feedback information for the synthesis of the superhard coating materials.

III. PROGRESS TO DATE

A. Synthesis of Superhard Materials

Work during this period was concentrated in four areas:

1. Synthesis of Various Carbides in the Ta-C System

The study on the synthesis of various carbides in the Ta-C system was completed and presented at the Conference on Structure/Property Relationships in Thick Films and Bulk Coatings in San Francisco, February 1975. The entire paper is included in Appendix I of this report.

2. Synthesis of Tungsten Carbides-WC_x.

a) The objective is to attempt to synthesize various carbides of the WC system through the evaporation of elemental Tungsten in the presence

of a reactive gas, i.e., high purity acetylene (C_2H_2) while employing the ARE process.

b) Experimental Procedure

i) Elemental tungsten was evaporated in the presence of high purity (99.6%) acetelyene. The ARE process was used during all runs.

ii) Various electron beam emission current levels were investigated and an emission current level of 1.03A in a 1" dia. pool was selected. This was the maximum power level of the electron beam gun used, i.e., 10 KW. Also, it should be noted that due to the very high melting point of W, an emission current level in excess of 1.35A was needed to produce a completely molten pool on top of the 1" dia. evaporant rod. The emission current of 1.03A produced a molten pool approximately 70% of the surface of the evaporant rod. This phenomena produced excessive cavitation of the evaporant rod, with the sides of the billet remaining solid, thus shadowing the pool more and more as the evaporation process proceeded. An attempt was made to alleviate this "Cratering" effect by employing an x-y sweep of the electron beam on the pool surface. It was not effective. The reason the x-y sweep was not effective was that in adjusting the y-direction, to completely cover the billet, the sweep in the x-direction would overlap the billet and strike the copper cooling jacket of the crucible. This is an inherent limitation of the equipment being used.

iii) Gas partial pressures were varied from 4×10^{-4} torr to 22×10^{-4} torr. Evaporation rates were varied from 3.17 g/min. to .404 g/min. to study the effect on deposit composition.

a') 2.2-2.4 μm was the maximum allowable working pressure attainable without employing the differential pressure barrier in the vacuum system, see Fig. 1.

9
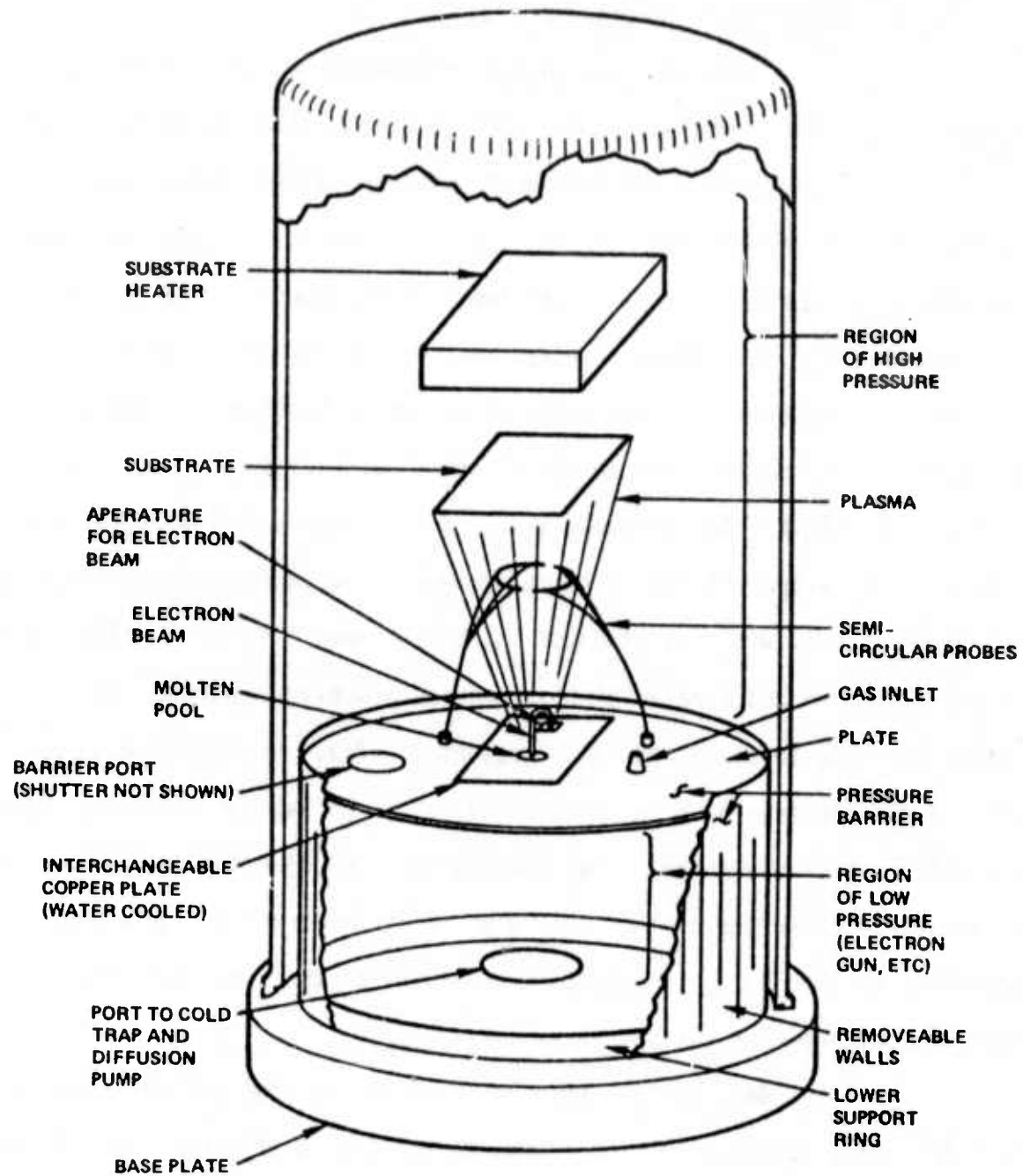
Figure 1. Section of Bell Jar — Revealing Essential System Features

10

b') 18-22 μm was the maximum allowable working pressure attainable while employing the differential pressure barrier with the port closed.

iv) Probe accelerating potentials between 10-20 V were used which resulted in observed probe current levels around 7A. However, it was noticed that the probe currents of up to 4A   e observed when tungsten was evaporated with the probe power supply voltage set at zero volts. This phenomena probably indicates the presence of large amounts of electrons emitted by the molten pool (W is a good thermionic emitter when heated) which might lead one to the conclusion that tungsten carbide could possibly be readily produced by Reactive Evaporation alone.

v) Characterization of the deposits was accomplished by x-ray diffraction, microhardness testing, metallography and the use of a Cambridge Scanning Electron Microscope.

vi) Substrate temperatures of approximately 1400°F were employed. The substrate materials were stainless steel and small pieces of alumina 1"x1"x1/8".

c. Results

Various carbides of the WC system were readily synthesized by the evaporation of elemental tungsten in the presence of acetelyene gas while employing the ARE process. The results of various experiments are given in Table II. The carbide synthesis seemed to follow the phase diagram as put forth by Storms[9], Fig. 2. However, only the high temperature forms of the carbides were observed, i.e., β-W_2C, $WC_{.6}$ (β-WC) and WC [It was very hard to differentiate between α-W_2C which is normally encountered and β-W_2C because the x-ray 2θ values were almost identical. However, in investigating

TABLE II

Deposition of Various Compounds in the W-C System

Run	Evap. Rate g/min	Cond. Rate g/min	Thick mil/min	Press. Torr	Probes V	Probes A	Emission Current A	Hardness 50gm	Hardness 100gm	Temp. °F	Deposit Morphology	Phase Present
W-A-1	1.706	.547	.039	8×10^{-4}	15	7	1			930		W_2C, possibly B-WC
W-A-2	3.17						1.35–1.40			1800 1300		W_2C-Bulk, Some possible B-WC
W-A-3	2.24	.630		10^{-4}	16	6	1.1–1.15	2336		1380	Small Domes Cracks	Mostly WC, Some B-WC and W_2C apparent
W-A-7	1.06		0.18	1.6–1.8	30	6	1.0			1220	Large Domes Adherent	$W_2C + B$-WC
W-A-8	1.992	.494	.069	8-8.4×10^{-4}	17	8	1.03		2716	1440	Adherent	70% W_2C, 30% WC
W-A-9	2.247	.717	.072	6×10^{-4}	15	7	1.03		2998	?	Adherent 0Δ	W_2C, W,
W-A-10	2.230	.581	.076	4×10^{-4}	8	8	1.03	2617		1490	Medium Domes (small) Adherent 0Δ	W_2C, W
W-A-11	1.693	.447	.074	7×10^{-4}	10	8	1.03	2350	2732	1420	Large Domes Adherent (very ductile)	very large amount of W_2C, some W
W-A-12	1.514	.414	.071	1.1–1.2	16	7	1.03	2715		1370	Large Domes	Mostly WC_6 (B-WC) and possibly some WC but very small
W-A-13	1.757			2.2–2.4	16	6	1.03	2804		1360	Small Domes Cracks *non-adherent	B-WC, possibly some W_2C or WC

12

W-C Deposition
(continued)

Run	Evap. Rate g/min	Cond. Rate g/min	Thick. mil/min	Press. Torr	Probes V	Probes A	Emission Current A	Hardness 50gm	Hardness 100gm	Temp. of	Deposit Morphology	Phases Present
W-A-14	1.579			18-22	21	6	1.03	1677		1390	Large Domes *non-adherent	b-WC, W$_2$C no apparent WC
W-A-15	.404			8.2x10^{-4}			.72	2996		1400	Small Domes Cracks *non-adherent	WC- say 20% b-WC or W$_2$C Bulk
											O W$_2$C in Deposit increased W-A-10 → W-A-9 → W-A-11	
											Δ W in deposit increased W-A-11 → W-A-9 → W-A-10	
											Max. pressure without barrier installed	
											* Non-adherent means that large cracks were observed with some flaking	

13

Sora (1965c)

Liquid

2710°

W + W₂C

W₂C

β - WC

2785°
2755°
2525°

α - WC + C

Rudy et al. (1966)

Liquid

2710 ± 5°

2735 ± 6°

2776 ± 4°

β - W₂C

α - W₂C

W + α - W₂C

WC₁₋ₓ 2720 ± 10°

2530 ± 20°
2450 ± 20°

α - W₂C + WC

WC + C

WC

Temperature, °C

C/W, atom ratio
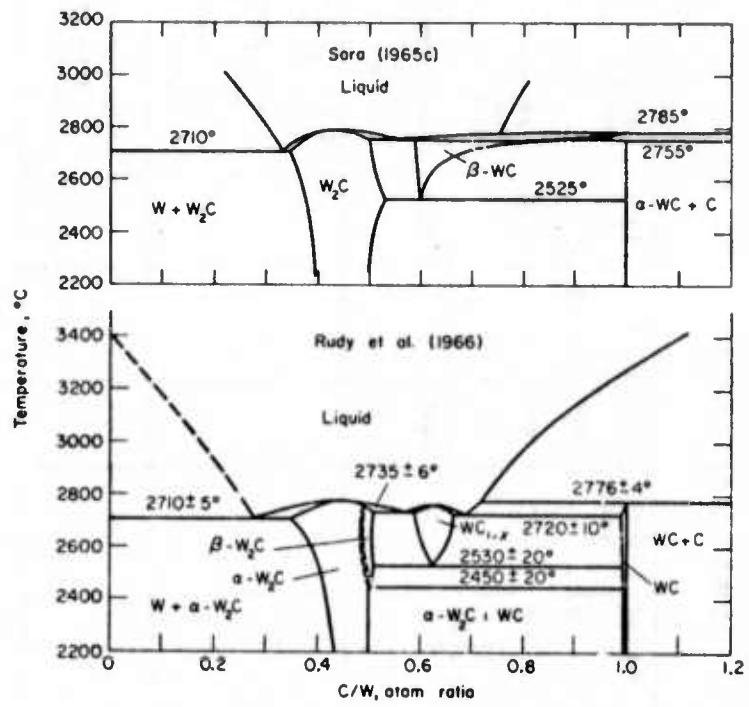
Figure 2: Two versions of the W-WC system
after Storms(9).

14

the higher 2θ values it appears as though $\beta-W_2C$ was present]. This anomaly seems quite surprising because the phase diagrams indicate that $\beta-W_2C$ decomposes to $\alpha-W_2C$ at 2450°C and that $\beta-WC$ is not stable below 2525°C. Therefore, it must be in metastable equilibrium at room temperature.

An explanation for the above anomaly seems plausible if the high temperature form of the carbides were formed in the gas phase which happens in the ARE process. Upon condensing on the heated substrate rapid cooling of the deposited species would occur, even though the substrate was at 750°C. This effect would then have hindered the dissociation of the incident molecular clusters and the subsequent surface diffusion of the atomic species, i.e., tungsten and carbon to form the low temperature species, resulting in an effective "freezing in" of the high temperature structure.

Increasing the acetylene partial pressure from 4×10^{-4} to 2.2×10^{-4} torr resulted in the sequential deposition of $W + W_2C$, $W_2C + WC$, $WC_{.6}$ and $WC_{.6} + WC$ (possibly small amounts of W_2C) with a fixed emission current level of 1.03A. However, for deposits synthesized at pressures greater than 1×10^{-3} torr, the deposits were partially non-adherent. This could have resulted from localized cracking of the deposit thereby reducing the large internal stresses introduced from thermal coefficient of expansion mismatch between the substrate and deposit. This effect can be reduced by decreasing the thickness of the deposit or producing a graded interface between the deposit and substrate.

Upon examination of the deposit morphology, large botroydal, or domed crystallites corresponding to a Movchan zone I structure. Takahashi, et al.[10] also observed this structure on CVD deposited tungsten carbide but at much higher substrate temperatures, i.e., 1360°C. In cross-section, however, an entirely different structure was observed.

Metallographic examination of the cross-section revealed several things (see Figs. 3,4,). The cross-section appeared to show an equiaxed, two-phase fine grain structure with a shallow diffusion layer between the deposit and substrate. This could have been the cause of the increased adherence of thick films deposited at acetylene pressures less than 1×10^{-3} torr. Also, a layered structure was observed on most deposits.(see Fig. 4). This observed layered structure probably represents small variations in composition (probe current was fairly constant during runs). Compositional variation could have occurred as "cratering" of the feed material became progressively worse during the evaporation of the tungsten. This would then have caused effective shadowing of the molten pool, decreasing its area and hence the supply of evaporant species to the gas phase per unit time.

The hardness of the deposits seems to fall within the 2250-3000 Kg/mm^2 range reported by Storms.[9] However, it is interesting to note that the deposits containing $W + W_2C$ showed hardnesses in the 2600-3000 Kg/mm^2 range which Storms attributed to mixtures of $W_2C + WC$. This is surprising in that appreciable amounts of W present in the W_2C deposit would be expected to lower its hardness. The possible reasons would be solid solution hardening of W by C or the hardening effect of an ultrafine grained two phase structure.

d. Conclusions

The feasibility of synthesizing the various carbides of the W-C system has been shown using the Activated Reactive Evaporation process, although the mono-carbide, WC, was not formed without other carbides being present.

3. Synthesis of Fine Grained TiC-Ni Cermet Deposits

a. Objective: The objective of this investigation is two fold.

16
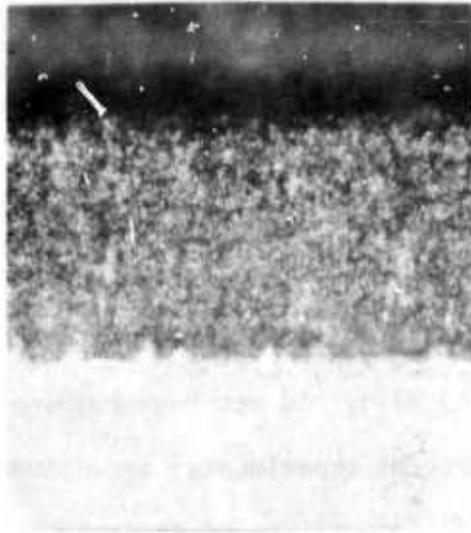
Deposit

Figure 3: Cross-section of deposit consisting
of a two phase, fine grained struc-
ture of W + W_2C.   (750X)
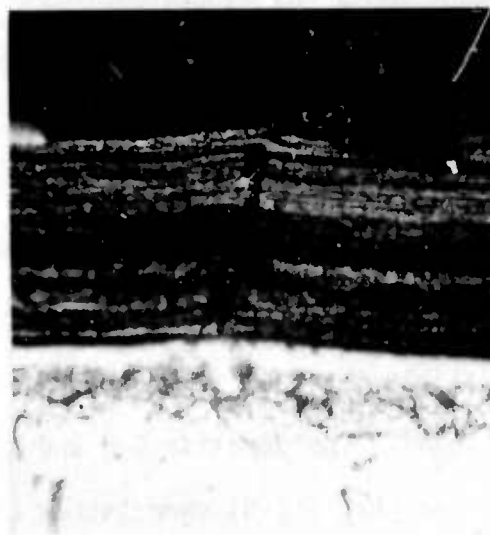
Figure 4: Deposit consisting of WC with some
β-WC and W_2C showing a layered
morphology.   (750X)

17

i) To make a feasibility study of synthesizing TiC-Ni cermets by the ARE process. Ti-Ni alloy will be evaporated from a single rod fed electron beam evaporation source in the presence of C_2H_2.

ii) To characterize the deposits by x-ray diffraction, micro-hardness measurement, electron microprobe analysis and optical and electron microscopy.

b. Synthesis of TiC-Ni Cermets

A Ti-Ni alloy rod has been evaporated in the presence of C_2H_2 gas in the ARE process experimental arrangement as described in the literature.[11,12] Temperature of deposition, evaporation rate of alloy and pressure of the reactive gas are the experimental variables. The experimental conditions for various deposits are summarized in Table III.

c. Characterization of the Deposits

The deposits were characterized by x-ray diffraction, micro-hardness measurement and x-ray fluoresence analysis using a Kevex unit attached to scanning electron microscope. The results are also included in Table III. X-ray diffraction patterns show that the deposits C-1 and C-2 are made up of TiC and Ti_2Ni and the deposits C-8 and C-9 consist of TiC and Ni. The possible explanation for this difference is the evaporation rate of the alloy. In the deposits C-1 and C-2 the evaporation rates are high and hence possibly there is some free Ti which did not form carbide and hence formed Ti_2Ni. The deposits C-8 and C-9 are the cermets of TiC-Ni. Thus this study shows that TiC-Ni cermets can be synthesized by ARE technique by controlling the evaporation rate and pressure of the reactive gas. The microhardness measurements were made with Knoop indentor using 50 g load and the values on the cermets (C-8 and C-9) indicate that these are quite hard.

18

Table III

Synthesis of TiC-Ni Cermets

Run	Emission Current A	Evap. Rate g/min	Reactive gas C2H2, press. torr	Dep. Temp. °C	Probe Voltage V	Probe Current A	Substrate Material	Micro-hardness KHN Kg/mm²	X-ray diffraction showed peaks of	Wt% of Ni as shown by Kevex
C-1	0.30	0.66	$7\text{-}8\times10^{-4}$	700	35-40	3-7	Stainless Steel	1830	TiC & Ti_2Ni	Not Analyzed
C-2	0.30	0.79	$8\text{-}9\times10^{-4}$	550	27.5-30	5-7	Stainless Steel	1760	TiC & Ti_2Ni	Not Analyzed
C-8	0.20	0.32	$1.2\text{-}1.3\times10^{-3}$	1000	35-45	0.5-10	Tantalum	2810	TiC & Ni	7.75*
C-9	0.20	0.21	$1.1\text{-}1.2\times10^{-3}$	700	35-40	3-10	Tantalum	2050	TiC & Ni	4.5*

* Not absolutely certain, has to be analyzed again

C-8 deposit was mounted in cross-section, given a metallographic polish and etched with a solution of 10 g potassium ferricyanide, 10 g potassium hydroxide and 100 ml water. The optical micrograph is shown in Fig. 5, which shows a fine grain unresolved structure and a diffusion zone (white region) at the interface between the substrate and the deposit. X-ray image pictures of this interface region between the TiC-Ni deposit and Ta foil substrate for the elements Ti, Ta and Ni were taken on an electron microprobe analyzer as shown in Fig. 6. These pictures show that Ni diffused into Ta foil and formed an intermetallic phase formation which corresponds to the white diffusion zone seen in Fig. 5.

d. Conclusions

The feasibility of synthesizing TiC-Ni cermets by the ARE process has been demonstrated. Partial characterization of deposits was done. Further characterization of these deposits with microprobe analyzer will be carried out. Replicas of these deposits are being made to observe in the transmission electron microscope to be able to resolve the fine grain size.

B. Machining Evaluation of Coated High Speed Steel Tools

The machining evaluation of uncoated and coated tools was initiated and the machining performance was examined. Turning operations on a 5" dia. workpiece of 4340 steel using high speed steel inserts (M43) with and without coatings were carried out. The machining tests were done at a speed of 150 rpm, a feed of 0.003"/rev., and a depth of cut of 0.050". The cutting forces were continuously recorded during the test. The results are shown in Table IV. A typical trend of the major cutting force for the uncoated M43 insert is shown in Fig. 7. At the start of the test, the cutting edge is in as-ground state. As cutting continues, the local temperature and the contact pressure between the cutting edge and the chip are high and finally, the tool fails by fracture

TABLE IV

Results of First Tests of Uncoated and Coated High Speed Steel Inserts

No.	Coating	Thickness	Tool Life	Increase in Tool Life	Force (arbitrary units)	Mode of Failure
M43	Uncoated		3 min.		1	Fracture of tool edge.
M43-1	TiC-10Ni	12 μm	11 min. 40 sec.	300%	0.5	Fracture of tool edge
M43-2	TiC-5Ni	5 μm	>12 min. 40 sec.	>330%	0.5	NO FAILURE (Test was stopped at the end of the workpiece)
M43-3	TiC	12 μm	12 min.	300%	1	Fracture of tool edge.

21
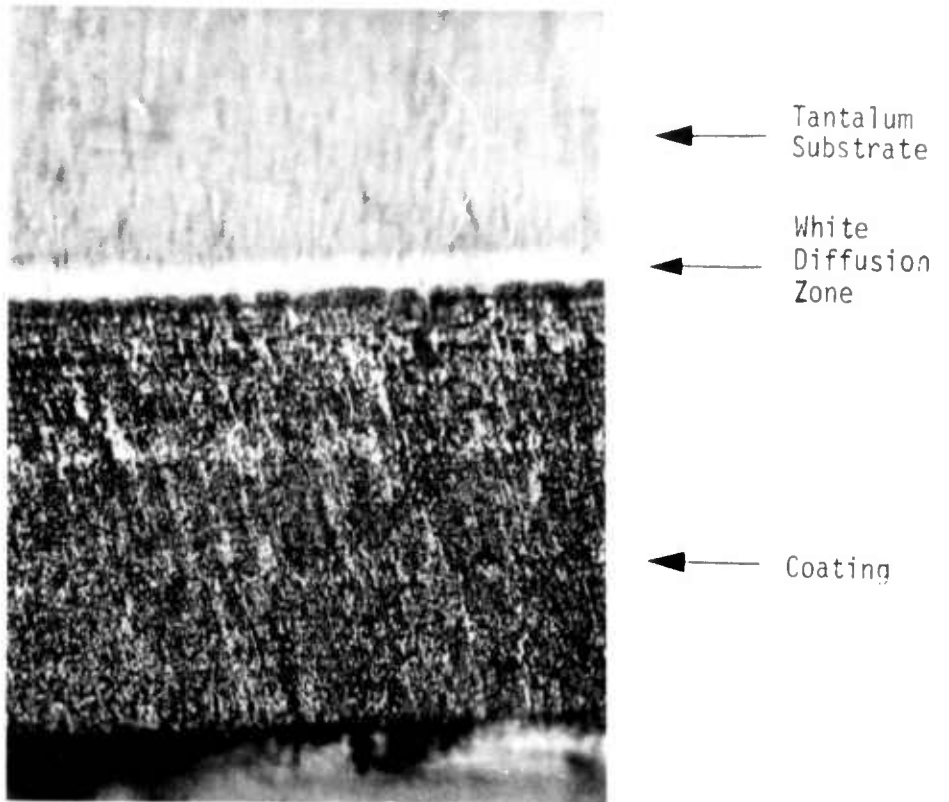
Figure 5: Optical Micrograph of Sample showing a fine grain TiC-Ni deposit, a diffusion zone (white) and Ta substrate. (1000X)
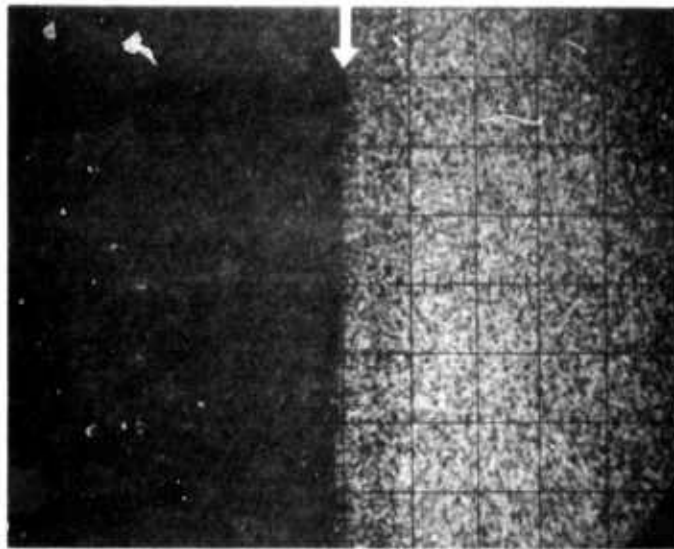
(a)   Ta
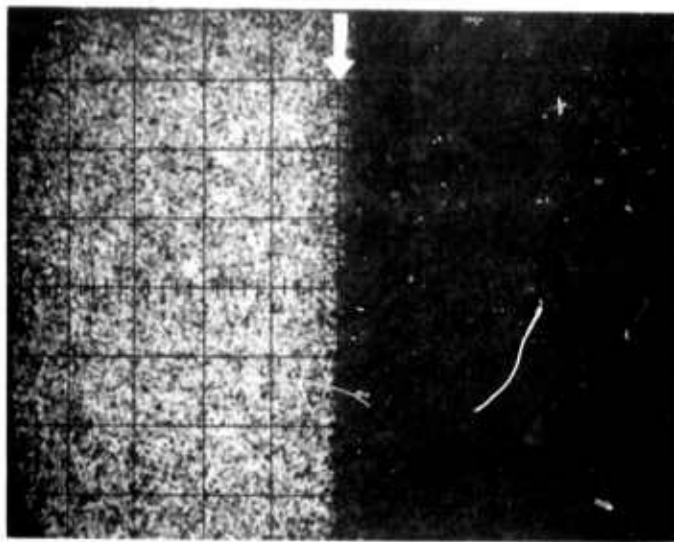
(b)   Ti
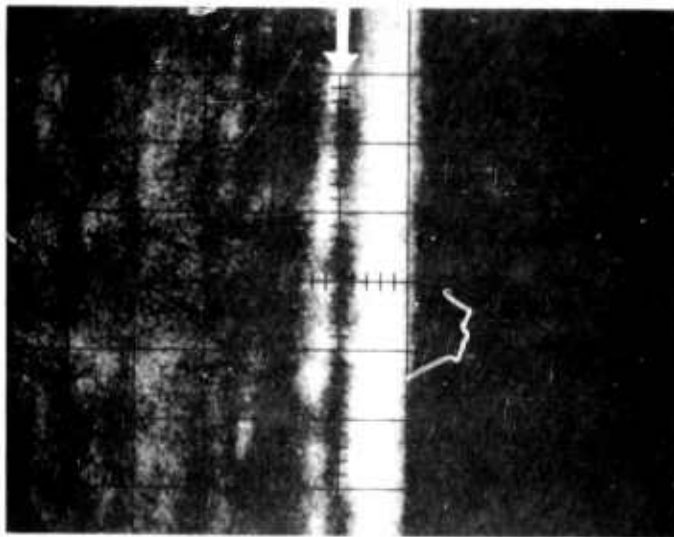
(c)   Ni

Figure 6:   X-ray maps of Sample C-8 for Ti, Ta, and Ni at the interface between Ta substrate and TiC-Ni deposit. There is a concentration of Ni at the interface on the Ta side.   (2000X)

23

of the cutting edge; chipping of the tool cutting edge occurs, as shown in Fig. 7. The total machining time is 3 minutes and 40 seconds in this case.

Figure 8 shows the major cutting force during machining with a coated M43-1 with the same cutting conditions of the uncoated tool. The coating is TiC-10Ni of the thickness of 5 μm. The cutting force and the tool tip temperature in this case are half that for uncoated tools. The machining test was stopped after covering the full length of the workpiece. The machining time in this case is 12 minutes and 40 seconds (about 4 times that of the uncoated) and with the cutting edge still unbroken (as shown in Fig. 8).

Another tool with a TiC-10Ni of thickness 12 μm exhibited cutting forces half that of the uncoated tool. The total machining time is 11 minutes and 30 seconds which is over three times that of uncoated tools. The failure mode was progressive wear of the coating leading to an increase in cutting force and ultimately fracture of the tool edge.

A fourth tool with a TiC coating 12 μm thickness showed a 12 min. tool life but without the decrease in tool force.

These initial results demonstrate the effectiveness of the coating in improving the performance of high speed steel tools. It is believed that by achieving a proper combination of coating material, microstructure and interface bonding improvement in tool life by a factor of 10 would be feasible. Continued development of superhard materials, examination of the tool substrate-coating interface, and machining evaluation of the coated tools are the main thrust of the future program.

24
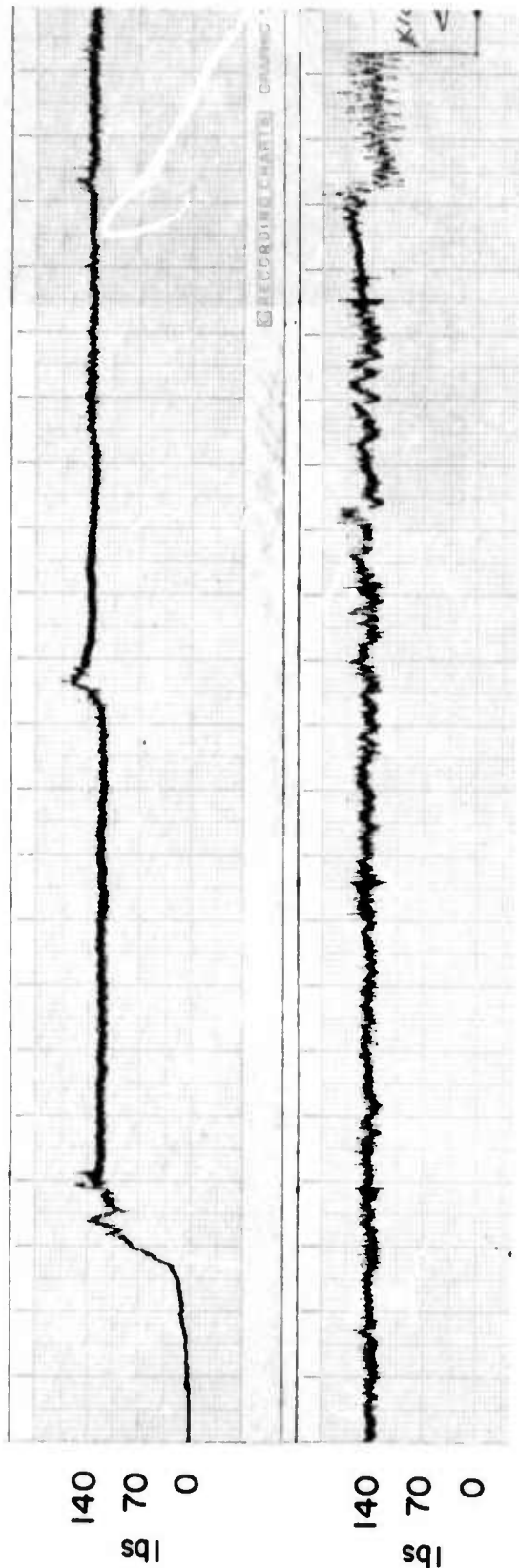
FRACTURE OF
CUTTING EDGE

Figure 7: Uncoated M43 Tool-Cutting Edge Fracture After
30 min 40 sec.

25
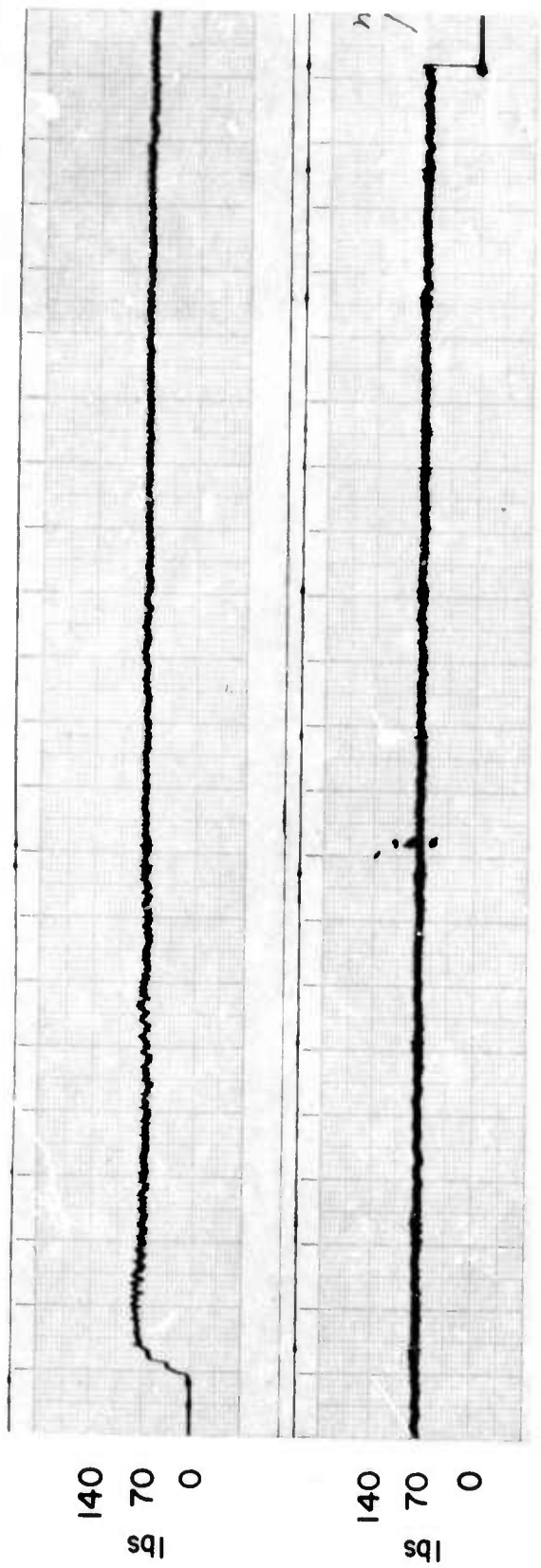
CUTTING WAS STOPPED BEFORE
FRACTURE OF CUTTING EDGE

Figure 8: Coated M43-1 Tool-Machining Stopped After
12 min 40 sec.

26

IV. FUTURE RESEARCH EFFORTS

The research effort in the next period will consist of:

1. Further development of the BARE process and its effect on structure and properties of carbides.

2. Continuation of the evaluation of TiC-Ni cermets and the interface with the substrate

3. Examination of the coated tools after machining.

4. Synthesis of TiC-VC mixed carbides.

5. Coating of high speed steel tool inserts and their machining performance.

27

REFERENCES

1. Auwarter, M. Blazers, Liechtenstein, U.S. Pat. 2,920,002, (1960).

2. Bunshah, R. F. and A. C. Raghuram, J. Vac. Sci. Tech. 9, (1972) pp. 1385-1388.

3. Bunshah, R. F., "High Rate Deposition of Carbides by Activated Reactive Evaporation", U.S. Pat. 3,791,852 (1974).

4. Hass, G. and E. Ritter, J. Vac. Sci. Tech. 4, No. 2, (1966), pp. 71-79.

5. Holland, L., "Vacuum Deposition of Thin Films", Chapman & Hall, Great Britain, (1966).

6. Maissel, L. I. and R. Glang, Handbook of Thin Film Technology, McGraw Hill, New York, New York, (1970).

7. Hodgkinson, I., J. Applied Optics, Vol. 9, No. 7, (July 1970), pp. 1577-1586.

8. Heitman, W., J. Applied Optics, Vol. 10, Nol 11, (Nov. 1971), pp. 2414-2418.

9. Storms, E. K., The Refractory Carbides, Vol. 7, Academic Press, New York (1967).

10. Takahashi, T. and Hideaki, I., Journal of Crystal Growth, Vol. 12 (1972) pp. 265-271.

11. Bunshah, R. F., "New Techniques for the Synthesis of Metals and Alloys", UCLA-ENG-7161, (Sept. 1971).

12. Bunshah, R. F. and Raghuram, A. C., J. Vac. Sci. Tech., 9, 1385, (1972).

SYNTHESIS AND MORPHOLOGY OF VARIOUS CARBIDES

IN THE TANTALUM-CARBON SYSTEM

W. Grossklauss and R. F. Bunshah
Materials Department
University of California at Los Angeles
Los Angeles, California   90024

ABSTRACT

Tantalum carbides, i.e. TaC and Ta_2C, were readily synthesized by evaporating elemental tantalum in the presence of acetylene gas. A high rate physical vapor deposition technique employing the activated reactive evaporation process was used. The C/Ta ratio of the TaC deposits was found to increase with increasing C_2H_2 partial pressure. The hardness of the TaC was 2482 kg/mm^2 KHN, which is comparable to the literature values while the hardness of Ta_2C was twice that previously reported. It was found that the morphology changed markedly with deposition temperature.

INTRODUCTION

Carbide films in recent years have become of increasing importance due mainly to their high hardness and consequent wear resistance. An example of this is TiC, whose hardness can be changed from 3000-5000 kg/mm^2 KHN by varying the deposition parameters as reported by Raghuram and Bunshah.[1] The purpose of the present work is to study the synthesis of various tantalum carbides by the activated reactive evaporation process (ARE).[2,3] and the effects of experimental parameters on the structure of the deposit.

The preparation of polycrystalline samples of carbides has been generally accomplished by the use of powder metallurgy techniques,[4] reduction of the metal oxide by carbon, direct reaction of metal hydrides with carbon, gas carburization,[5] and chemical vapor deposition,[6,7] These processes involve reactions such as the following:

$$TaCl_5 + C_xH_y + nH_2 \rightleftharpoons TaC + 5 HCl + C_{x'}H_{y'},$$

Good reviews are presented by Storms[4] and Toth.[8] However, all of the above processes require high substrate temperatures of between 1000°C - 2200°C. Recently, Darolia and Archibold[9] have produced fully dense ZrC carbides by arc melting techniques. Extensive post anneal heat treatments were however necessary to homogenize the as-cast dendritic structure inherent in such processes.

Using the ARE process, Raghuram, et al.[10,1] have prepared thick films of TiC, ZrC and (Hf-3Zr)C. However, the synthesis of tantalum carbide by reactive evaporation or sputtering does not seem to have been investigated.

33

The tantalum-carbide system has three stable phases Ta_2C, ζ-TaC and TaC,[4] (see Fig. 1). This work therefore differs from previous work in that we are synthesizing compounds in a metal-carbon system with more than one stable carbide, as opposed to such systems such as Ti-C where only one stable carbide, TiC, exists albeit with a wide homogenity range, $TiC_{1-0.65}$. The synthesis of the various tantalum carbides was accomplished by evaporating elemental tantalum in the presence of acetylene. The C/Ta ratio and hardness of the deposit were varied by adjusting the C_2H_2 partial pressure. The effects of deposition temperature upon the structure of the deposit was then investigated.

EXPERIMENTAL PROCEDURE

The general experimental techniques and apparatus used in the present work have been discussed in an earlier paper by Grossklaus, et al.[11] Basically, tantalum is evaporated from a rod-fed electron beam heated source with activation and/or ionization of the reactive species, in the presence of a reactive acetylene gas (i.e. the ARE process). The acetylene partial pressure and substrate temperatures were then varied to produce the desired carbide film.

The basic synthesis work was carried out in a vacuum system with a base pressure of 2×10^{-6} torr. In part of the work, installation of a differential pressure barrier was necessary to allow the use of the electron gun at pressures greater than 2×10^{-3} torr; this effectively lowers the pumping speed in the reaction zone.

The substrate material consisted of either 302 stainless steel or molybdenum which was mounted 6 inches above the molten pool. Deposition temperatures were varied from 550°C-1490°C. Heating was accomplished by using a direct

34
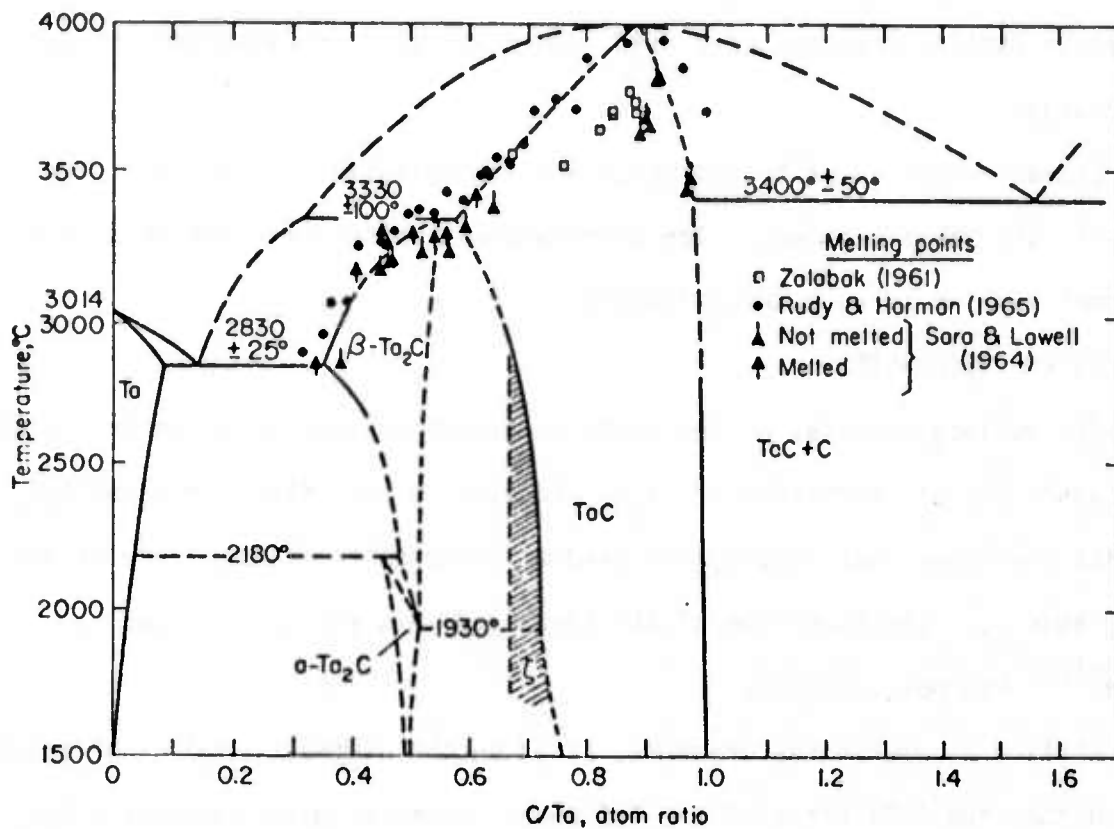
Fig. 1   Phase diagram of the Ta-C system according to Storms evaluation.[4]

resistance heated Mo foil for temperatures greater than 600°C and a radiant heater using tungsten filaments for temperatures below 600°C.

Tantalum evaporation rates were 1.0-1.39 g/min. The acetylene partial pressure was then varied in small increments from 4×10^{-4} torr to 8.8×10^{-3} torr. When varying the substrate temperature from 550°C to 1490°C, a fixed acetylene partial pressure of 8.8×10^{-4} torr was used to determine changes in morphology.

Characterization of the deposits was accomplished by x-ray diffraction analysis and SEM microscopy. The microhardness values were measured on a Micromet machine using a Knoop indentor.

RESULTS AND DISCUSSION

The various carbides of the tantalum-carbon system, as given by Storms[4], were synthesized. Formation of Ta_2C, changing to TaC with increasing C_2H_2 partial pressures, was readily achieved at a deposition temperature of 550°C (see Table 1). The formation of the so-called zeta phase, as shown by Brize[12], was not observed.

Lattice parameter measurements, based on the diffraction data of Storms[4], showed that the C/Ta ratio of the TaC phase increased with increasing C_2H_2 partial pressure (carbon content) from 7×10^{-4} torr to 1×10^{-3}. At pressures above 1×10^{-3} torr, introduction of the pressure barrier became necessary for stable operation of the electron beam gun. This resulted in an initial drop in the lattice parameter of the TaC deposit. This behavior was probably caused by the accumulation of excessive amounts of H_2 gas which could not have been pumped away fast enough from the reaction zone due to an effective lowering of the throughput, i.e. the rate of gas removal. As a result, the reaction $2\ Ta + C_2H_2 \rightarrow 2\ TaC + H_2$ is partially reversed; this results in a lower C/Ta ratio in the TaC deposit. Similar observations have been made in the synthesis

36

VARIATION OF MICROHARDNESS, LATTICE PARAMETER AND ORIENTATION OF TaC_x
DEPOSITED BY THE ARE PROCESS AT 500°C

TABLE I

Acetylene Partial Pressure (torr)	Deposit Formed	Lattice Parameter (Å)	C/Ta	Microhardness Kg/mm² KHN (50 gm)	Orientation [HKL]
4×10^{-4} *	Ta_2C	---	---	2442	{101}
$5\text{-}6 \times 10^{-4}$ *	Ta_2C	---	---	1907	{101}
7×10^{-4} *	TaC	4.431	.91	2287	{111}
8.4×10^{-4} *	TaC	4.449	.95	2482	{111}
1.0×10^{-3} *	TaC	4.453	.97	1800	{111}
2.0×10^{-3} *	TaC	4.449	.91	---	{111}
8.8×10^{-3} *	TaC	4.453	.97	---	{111}

* probe voltage 30 V and probe current 5A

37

of TiC when high pressures were used by the present investigators. This problem was eliminated by pumping separately above and below the pressure barrier.

The hardness of the tantalum carbide varied with C_2H_2 partial pressure, which governs the carbon content, and exhibited a maximum value at $C/Ta = .95$ of 2482 Kg/mm^2 for TaC. This hardness seems to be consistent with that reported in the literature[4,8], however, the literature values placed the maximum at $C/Ta = .83$. The lattice parameter values and consequent C/Ta ratios observed in the present work, could have higher values than those in the literatrue for several reasons. One possibility is the effect of the impurity content the deposited material, e.g. O, H, N. It is probably lower in the deposited material sintered powder specimens reported in the literature. This phenomena has been observed by Nickel, et al.[13] who showed the variation of CVD synthesized ZrC lattice parameters with oxygen content. Also, Ko, et al.[14] report that Ta absorbs large quantities of H_2 even at $78°K$.

The Ta_2C synthesized in this work, with a hardness of 2493 Kg/mm^2, is higher than Ta_2C previously reported,[4] (i.e. around 1000 Kg/mm^2). This high hardness may have resulted from the formation of super lattices or domain structures as discussed by Venables[15] or could have resulted from the formation of a mixture of Ta_2C and TaC. Storms[4] has observed that mixtures of WC and W_2C give hardness values that are higher than for either WC or W_2C alone. Mixture formation, however, was not detectable by x-ray diffraction analysis due to excessive peak brodening of the Ta_2C Bragg peaks, possibly associated with large internal stresses or small grain size. Thus, even if TaC were present, only Ta_2C peaks would be observed due to peak overlap.

When thick films are deposited at various deposition temperatures, one would expect a change in morphology as observed by many authors.[16-19] Movchan and Demchishin[18] have proposed just such a structural model. Their model consists of three structural zones. The transition from Zone 1 to Zone 2 occurs at 0.25 T_m for oxides and 0.30 T_m for metals, T_m being the melting point of the evaporated material in °K. Zone 1 consists of a domed or botroydal surface, and exhibits tapered crystallites in cross-section. Metals deposited with the Zone 1 structure are less than fully dense and show high strength but low ductility. Zone 2 which from 0.30 to 0.45-0.50 T_m, shows an equiaxed surface morphology with columnar grains in the cross-section. Metal deposits with Zone 2 morphologies have properties approaching those of cast materials, and occasionally have poor corrosion resistance due to intergranular corrosion. Zone 3 exists at $T \geq .50 \ T_m$ these deposits exhibit an equiaxed structure in the surface and cross-section, high ductility and good corrosion resistance but low strength, corresponding to that of annealed material. However, Thornton[20] has shown that these zone classifications are not ab absolute and that there is a transition structure between Zone 1 and Zone 2 which is ill defined. This transition zone consists of tightly packed fibrous grains.

The tantalum carbide thick films synthesised at deposition temperatures between 550°C and 1200°C showed a Movchan Zone 1 morphology. The deposits had a domed or botroydal structure, and the size of the crystallites increased with increasing temperature (see Figs. 2a-2d). This structure seems predictable, in that as the temperature is increased, the adatom surface mobility increases. This enables "clusters" of atoms to coalesce and grow. However, at these temperatures bulk diffusion is still very low, i.e. surface diffusion is apparently the predominating mechanism.
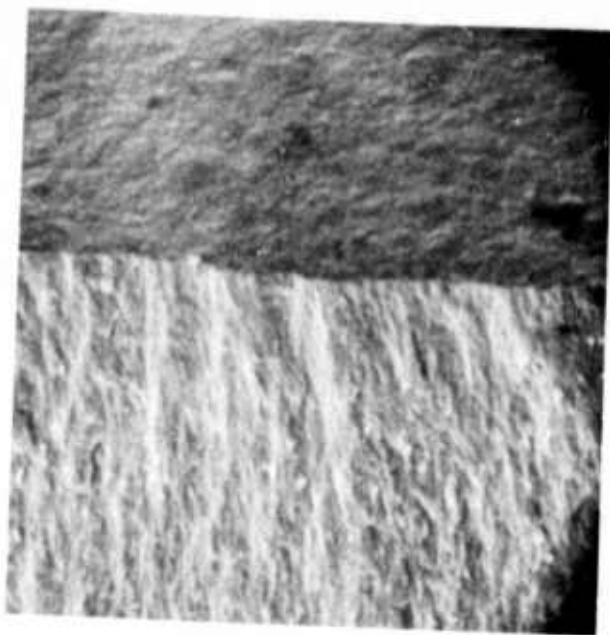
Fig. 2a. SEM photomicrograph of a TaC deposit surface and fracture cross-section at 550°C, ARE, showing small comed crystallites with zone 1 morphology. 3800X
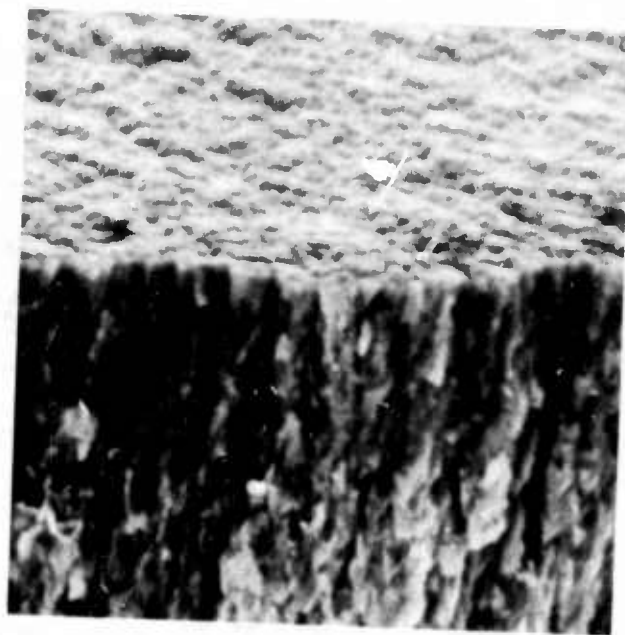

Fig. 2b. SEM photomicrograph of a TaC deposit surface and fracture cross-section at 930°C, ARE, showing crystallite growth and fibrous cross-section. 4300X
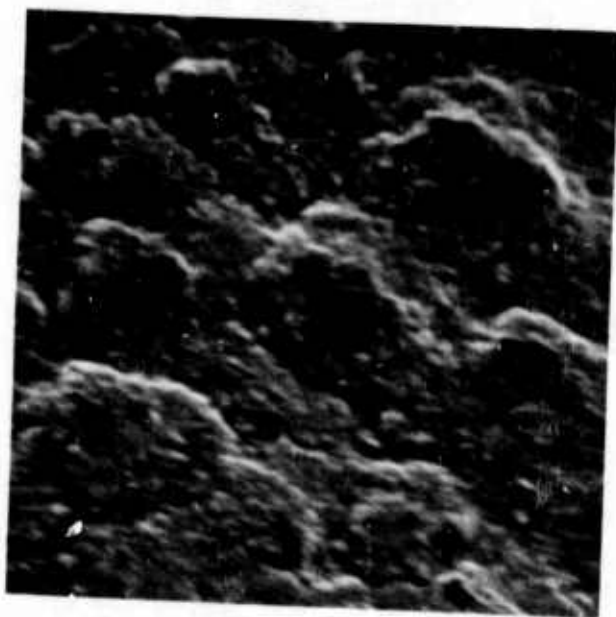

Fig. 2c. SEM photomicrograph of a TaC deposit surface at 1200°C, ARE, showing massive crystallites due to coalescence and growth. 3300X
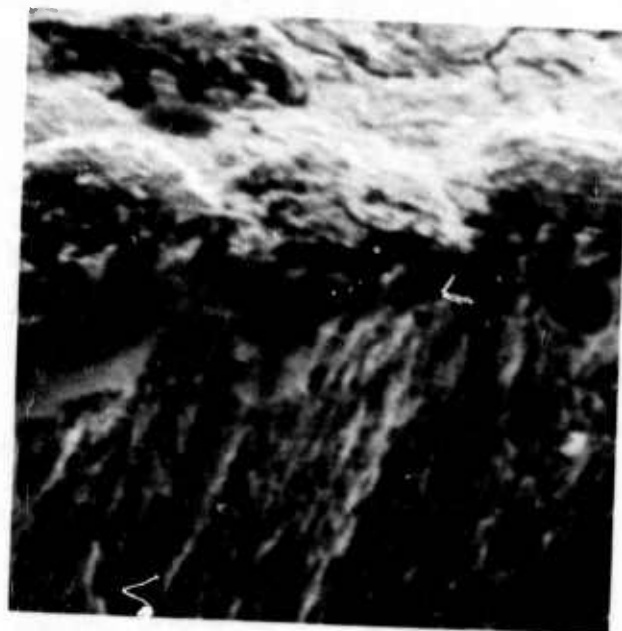

Fig. 2d. SEM photomicrograph of a TaC deposit fracture cross-section, 1200°C, ARE, showing large tapered crystallites. 3400X

Deposits synthesized at temperatures above 1200°C exhibit an entirely different morphology (see Figs. 3a-3c). At 1380°C, the deposit shows a morphology corresponding to one evolving from Zone 1 to Zone 2; some thermal faceting is visible. While at 1490°C, the morphology clearly shows a Zone 2 structure; the surface topography consists of thermally faceted, equiaxed grains, and a cross-section of columnar grains. This structure would now seem to indicate an appreciable amount of bulk diffusion and greatly increased adatom surface mobility. The Movchan-Demchishin model predicts a transition for TaC between Zone 1 and Zone 2 at 800°C; however, this transition was not observed. The transition to a zone structure did not start until 1200°C, the fully evolved Zone structure was realized at 1490°C. Thus, the interval between 1200°C and 1490°C appears to be a transition zone. Thornton[20] has attributed this tendency toward low temperature structures to the fact that absorbed gases limit adatom surface mobility. Also, such considerations as the binding energy between an atom and the bulk deposit may be a factor.

Crystallographic orientations of the tantalum carbide deposits were investigated by x-ray diffraction analysis. All deposits showed some preferred orientation. Deposits of Ta_2C were oriented with the (101) plane parallel to the deposition surface while TaC had a (111) orientation (see Table 1). It should be noted that the (111) plane, exhibiting extensive plastic flow as shown by Rowcliffe and Hollox[21], is the chief slip plane for TaC. This orientation could considerably affect the mechanical properties of the deposit since it also places the most densely populated atomic plane parallel to the surface of the deposit.

41
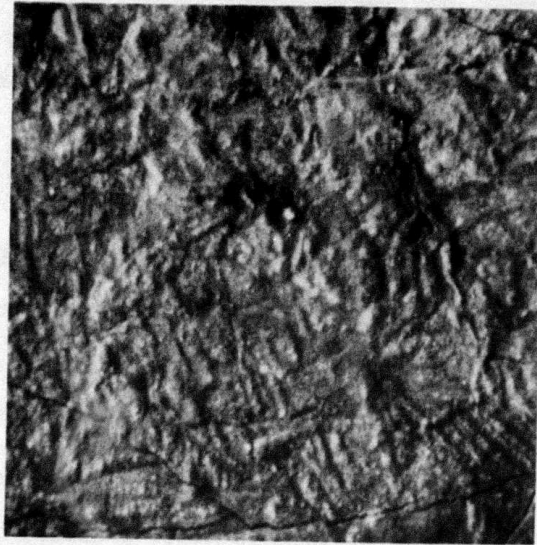
Fig. 3a. SEM photomicrograph of a TaC
deposit surface at 1380°C, ARE, showing
a transition structure from a zone 1 to
a zone 2 morphology and onset of thermal
etching. 1500X
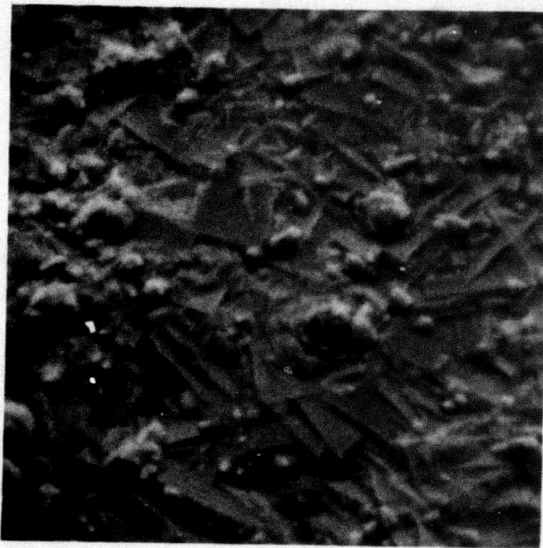
Fig. 3b. SEM photomicrograph of a TaC
deposit surface at 1490°C, ARE, showing
faceted, thermally etched, equiaxed
grains indicating a zone 2 structure.
7300 X
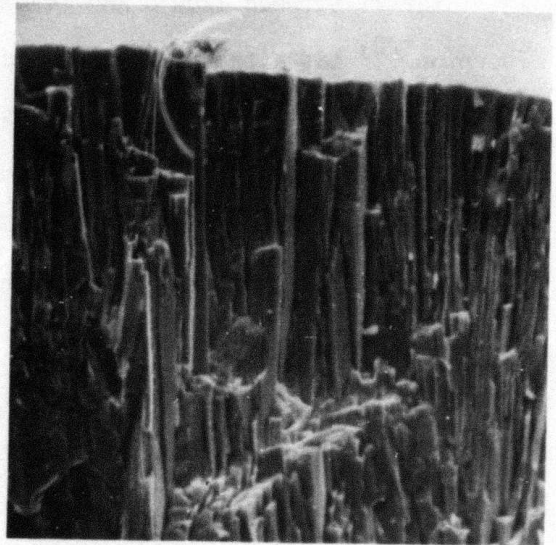
Fig. 3c. SEM photomicrograph of a TaC
deposit fracture cross-section at 1490°C
ARE, showing a fine columnar structure,
fractured transgranularly. 4800X

CONCLUSIONS

Using the ARE process, tantalum carbide films (i.e. Ta_2C and TaC) were readily synthesized by evaporating elemental tantalum in the presence of acetylene. It was found that marked changes in morphology occur with deposition temperature. Also, such parameters as the C/Ta ratio and hardness could be controlled by varying the C_2H_2 partial pressure. The hardness of the TaC formed was comparable to that previously reported in the literature, while the Ta_2C had twice the previously reported value.

ACKNOWLEDGEMENTS

REFERENCES

1. Raghuram, A.C. and R.F. Bunshah, J. Vac. Sci. and Tech., 9, 1389 (1972).

2. Bunshah, R.F. and A.C. Raghuram, J. Vac. Sci. and Tech., 9, 1385 (1972)

3. Bunshah, R.F., U.S. Patent No. 3,791,852 (1973).

4. Storms, E.K., The Refractory Carbides, Vol. 7, Academic Press, New York, (1967)

5. Johansen, H.A., Planseeberichte Fur Pulvermetallurgie, 18, 16 (1970).

6. Lee, M. and M.H. Richman, J. Electrochem. Soc., 120, 993 (1973).

7. Takahashi, T. and K. Sugiyama, J. Electrochem. Soc., 121, 714 (1974).

8. Toth, L.E., Transition Metal Carbides and Nitrides, Academic Press, New York, (1971).

9. Darolia, R. and T.F. Archbold, Metallography, 6, 433 (1973).

10. Raghuram, A.C., R. Nimmagadda, R.F. Bunshah, and C.N.J. Wagner, Thin Solid Films, 20, 187 (1974).

11. Grossklaus, W.D. and R.F. Bunshah, to be published, Jan-Feb. (1975) issue of J. Vac. Sci. and Tech.

    Auwarter, M., U.S. Patent No. 2,920,002, (1960).

12. Brizes, W.F. and J.M. Tobin, J. Am. Cer. Soc., 50, 115 (1967)

13. Nickel, H., O. Ione and K. Lucke, Z. Metallkunde, 59, 435 (1968).

14. Ko, S.M. and L.D. Schmidt, J. Vac. Sci. and Tech., 10, 294 (1973)

15. Venables, J.D. and M.Y. Meyerhoff, Nat. Bur. of Stand. Sp. Publ. 364, Solid State Chemistry, Proceedings of 5th Materials Research Symposium, issued, 583, (July 1972).

16. Bunshah, R.F. and R.S. Juntz, Metall. Trans. 4, 21 (1973).

17. Kennedy, K. Trans. Intr. Vac. Met. Conf., American Vacuum Society, 195 (1968).

18. Movchan, B.A. and A.V. Demchishin, Phys. Metals Metallog. (USSR), 28, (1969) p. 653 (English Translation, p. 83).

19. Neirynck, M., W. Samaey and L. Van Povcke, J. Vac. Sci. and Tech., 11, 647 (1974).

20. Thornton, J.A., J. Vac. Sci. and Tech., 11, 666 (1974).

21. Rowcliffe, D.J. and G.E. Hollox, J. Mat. Sci., 6, 1261 (1971).